

ICSO 2016

International Conference on Space Optics

Biarritz, France

18–21 October 2016

Edited by Bruno Cugny, Nikos Karafolas and Zoran Sodnik



***Design and tests of the sun baffle for the Sentinel-4 UVN
embedded calibration assembly***

L. Clermont

P. Blain

E. Mazy

J. Y. Plesseria

et al.



icso proceedings



DESIGN AND TESTS OF THE SUN BAFFLE FOR THE SENTINEL-4 UVN EMBEDDED CALIBRATION ASSEMBLY

L. Clermont¹, P. Blain¹, E. Mazy¹, J.Y. Plessier¹, B. Marquet¹, Y. Stockman¹
¹Centre Spatial de Liège (CSL), University of Liège, Avenue du Pré Aily, Liège, Belgium;

I. INTRODUCTION

The Sentinel-4 mission (S4) is part of the Global Monitoring for Environment and Security (GMES) initiative and covers the needs for continuous monitoring of Earth atmospheric composition and air pollution [1]. Sentinel-4/UVN is one of its instruments, a high resolution spectrometer operating in 3 spectral domains: UV (305-400nm), VIS (400-500nm) and NIR (750-775nm). A sketch of UVN is presented on Figure 1.

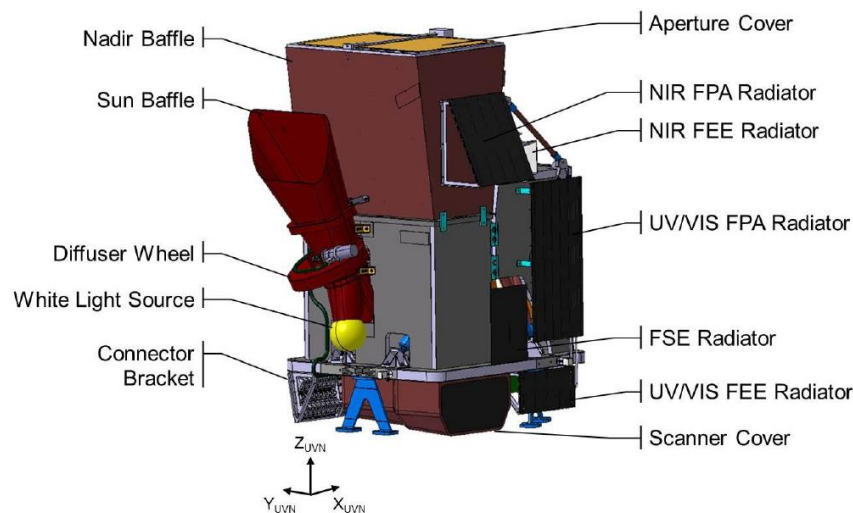


Figure 1: Overview of UVN instrument and the calibration assembly (CAA)

The radiometric accuracy of the UVN instrument partly relies on regular in-orbit re-calibrations: the goal is to determine, for example, the sensor gain factors and their drifts due to aging and exposition to operation conditions. One of the in-flight calibration approaches consists in the measurements of the sun's irradiance as transmitted by a diffuser. Thanks to a diffuser wheel, several diffusers can be used to cross-check the calibration in case the diffuser performance would drift too. The calibration assembly (CAA) includes a sun baffle, which ensures the stray-light rejection for the sun calibration. This paper presents the design and stray-light analysis of the baffle, as well as its experimental testing.

II. DESIGN

The goal of the sun baffle is to block earth shine and to provide a sun stray-light below 0.2% inside the UVN field of view ($\pm 2.1^\circ \times \pm 0.1059^\circ$). The sun calibration is performed regularly and for directions included inside the field of view (FOV) defined by the 4 direction cosines vSun of Table 1. Based on these constraints, the baffle was designed; respectively $\pm 0.27^\circ$ and $\pm 8.74^\circ$ angular divergence for the sun and earth illumination were considered. Figure 2 shows a picture of the sun baffle and a 3D sketch extracted from the ray-tracing software FRED. Because the earth position relative to the instrument is fixed, the baffle is asymmetric with the larger part on the side of the earth (Figure 3-a).

	X	Y	Z
vAxis	0,374705	-0,203129	-0,904618
vSun1	0,381322	-0,431141	-0,817747
vSun2	0,308599	-0,431141	-0,847870
vSun3	0,341790	0,036644	-0,939062
vSun4	0,422334	0,036644	-0,905699
vEarth	0	0	-1

Table 1: Direction cosines of the sun baffle optical axis, extreme sun illumination fields and earth illumination (global UVN reference frame)

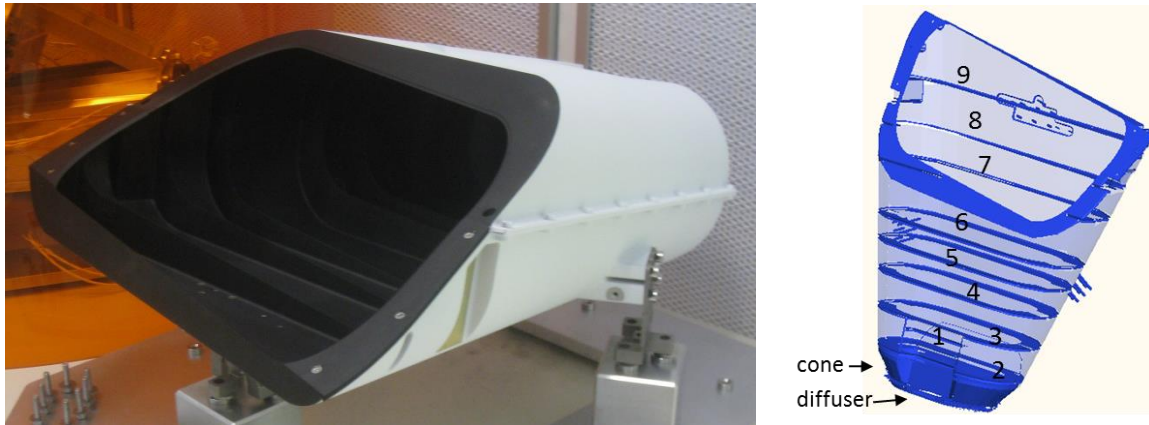


Figure 2: Picture and sketch of the sun baffle.

The vanes were designed such that they minimize the surfaces of the baffle which are at the same time seen from the scene (i.e. illuminated) and seen from the diffuser (i.e. critical) [2]. Indeed, these are the surfaces responsible for 1st level stray-light. Figure 3-b shows the surfaces of the baffle which are seen from the diffuser, while Figure 3-c and d shows surfaces illuminated by the sun for respectively configuration vSun2 and vAxis. As these figures show, the bottom cone of the baffle remains both illuminated and critical, especially for fields away from the optical axis (here vSun2). Furthermore, this is also true for a small wall at the bottom of the baffle that had to be made in order to hide the mechanical structure of the diffuser wheel.

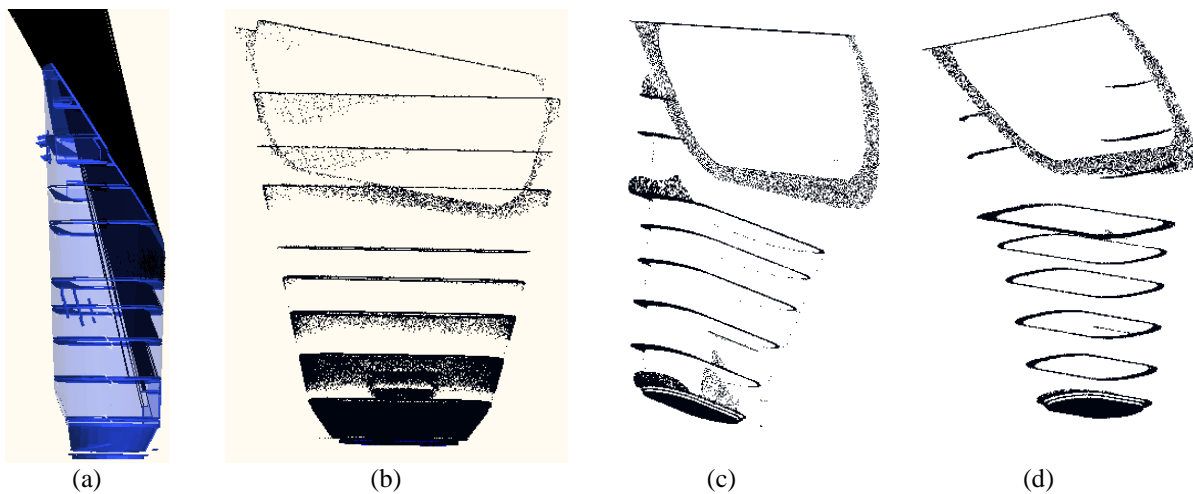


Figure 3: Sketches extracted from the non-sequential ray-tracing software FRED (a) Earth illumination ray tracing. (b) Surfaces of the baffle visible from the diffuser (i.e. critical surfaces). (c) and (d): surfaces illuminated by the sun for configuration vSun2 and vAxis respectively.

III. ANALYSIS

A. Methods

The stray-light rejection performance of the baffle was assessed using the non-sequential ray-tracing software FRED. By definition, the stray-light at Nth scattering level is expressed as the ratio of the irradiance at Nth scattering level divided by the direct sun irradiance, where level Nth means that the light is scattered N times before hitting the detector.

$$\text{Straylight @ } N^{\text{th}}\text{level} = \frac{\text{Irradiance @ } N^{\text{th}}\text{level}}{\text{Direct sun irradiance}}$$

The performance of the baffle was simulated at scattering level 1 and not considering the edges of the vanes. As the illuminated surfaces of the baffle vary when the field is varied, the stray-light was investigated for several fields inside the FOV (Figure 5-right). The stray-light induced by scattering on the edges of the vanes was investigated separately, as their very small size requires that rays are sent specifically on them to obtain a good statistic. The edges simulations were done for all of the extreme fields, from vSun1 to vSun4 (Table 1). Finally, the impact of the stray-light due to retro-diffusion of direct light on the diffuser was investigated.

The analysis was performed by calculating the stray-light at diffuser level. This is a conservative assumption as in practice the stray-light is scattered by the diffuser and only a portion of it actually goes inside the field of view of the instrument. Thus, this gives an over-estimation of the stray-light level. The assumptions were then made less conservative by considering the angular distribution of the stray-light and introducing experimental measurements of the diffuser in the model.

One of the goals of the analysis was to perform a trade-off on the coating to be used. Two coatings were investigated: Acktar and inorganic black anodization (Figure 4). The second one is more specular but presents less constraints of manufacturability than Acktar. A hybrid configuration was considered where black anodization is used everywhere except for the bottom of the baffle, the cone, where acktar is used instead. This is motivated by the analysis of illuminated and critical surfaces which has shown that the most probable source of stray-light comes from that cone.

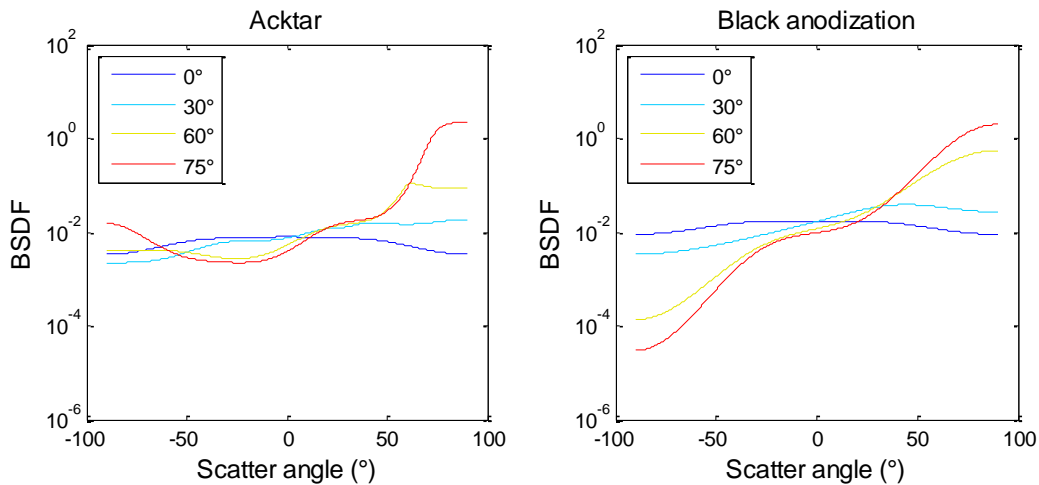


Figure 4: BSDF for acktar fractal black (left) and black anodization (right), defined in FRED based on experimental datas

B. Results

Figure 5-left shows the 1st level stray-light of the baffle, edges not included, as a function of the illumination configuration. The three coatings situations are presented; black anodization gives the highest level of stray-light while acktar improves significantly the rejection performance of the baffle. The performance of the hybrid coating is very close to the acktar case, as most of the stray-light comes from the cone which is also coated with acktar in hybrid case. Furthermore, the figure shows that the most critical illumination configurations happen for fields on the side of vSun3 and vSun2; this is explained by the fact that the wall hiding the wheel mechanical structure is the most visible from these angles.

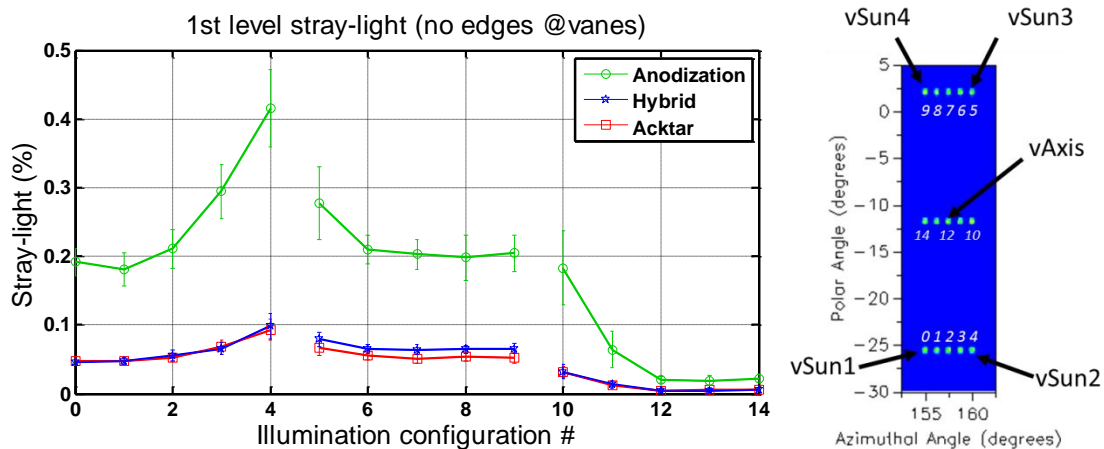


Figure 5: (left) 1st level stray-light @diffuser level, due to the direct sun illumination on the baffle, excluding the effect of vanes edges. (Right) Illumination configuration (UVN global reference frame)

Figure 6 shows the stray-light impact of the different edges of the vanes, considering either black anodization or acktar coating. The number of the edges relates to the labels on Figure 2-right. The shape of the curve is the result of two competing effects: vanes further from the diffuser have a larger illuminated surface but a smaller view factor from the diffuser. These curves were obtained considering a flat edge with bevel at the tip of each vane. The flat edge was defined with a thickness of 200µm, in agreement with mechanical and coating deposition process constraints. These results can however be used to derive the edge-induced stray-light for edges with a different thickness provided a simple scaling.

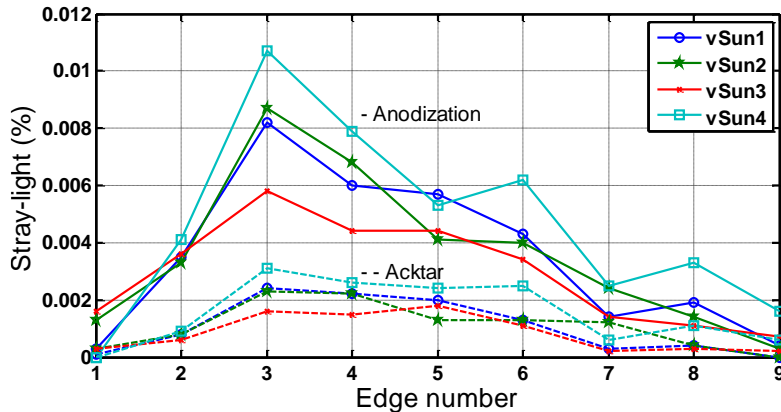


Figure 6: 1st level stray-light @diffuser level, due only to direct illumination on the vanes edges. Continuous and dotted curves are respectively the case of black anodization and acktar coating.

When light is retro-diffused on the diffuser, scattering on the sun baffle can cause additional stray-light. The difficulty of its modeling was to define the properties of the diffuser; several cases were thus analyzed considering a diffuser with lambertian emission over different emission angles (Figure 7-right). Based on the experimental characterization of the hemi-reflectance (Figure 7-left), a fixed hemi-reflectance of 30% was selected as a conservative assumption. As Figure 7-right shows, the anodization and hybrid coating give similar results for small emission angle as in this case the main contributor to stray-light are the vanes of the baffle (both in black anodization). For higher emission angles, the cone becomes responsible for more stray-light and thus the hybrid case is better than anodization.

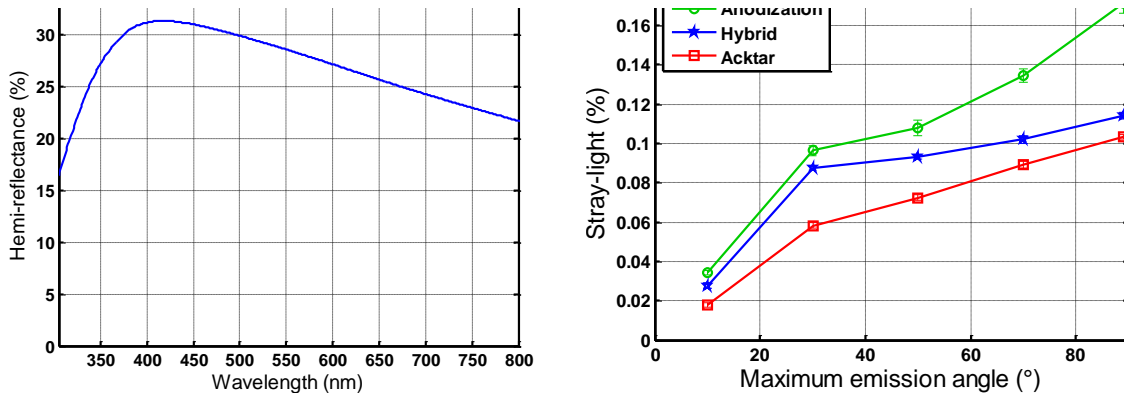


Figure 7: (Left) Hemi-reflectance of the diffuser. (Right) Stray-light due to retro-diffusion on the diffuser

The results above, summarized in Table 2, were obtained with very conservative assumptions. One of them is that stray-light is calculated at diffuser level, without restriction on the incidence angle of the stray-light on the diffuser. In practice, however, light hitting the diffuser with large incidence angles will mostly fall out of UVN field of view. This was demonstrated experimentally, as shown on Figure 8-left. This experimental result was used as a weight factor to calculate more accurately the stray-light, considering the worst illumination condition vSun2. The method consisted in measuring the angular distribution of the stray-light on the diffuser. The result was then multiplied by the weight factor to keep only the stray-light going inside UVN FOV. For example, Figure 8-right shows the angular distribution of the stray-light due to direct illumination, edges excluded (hybrid coating). The gross data as well as the data multiplied by the weight factor are presented. By the end, for hybrid coating configuration, stray-light is reduced by a factor of about 1.5 when considering the angular weight factor.

	Acktar				Black anodization				Hybrid			
	vSun1	vSun2	vSun3	vSun4	vSun1	vSun2	vSun3	vSun4	vSun1	vSun2	vSun3	vSun4
Direct sun illumination - no edges	0.05%	0.09%	0.07%	0.05%	0.19%	0.42%	0.28%	0.21%	0.05%	0.10%	0.08%	0.07%
Direct sun illumination - edges only	0.01%	0.01%	0.01%	0.01%	0.03%	0.03%	0.03%	0.04%	0.03%	0.03%	0.03%	0.04%
Total direct sun illumination	0.06%	0.10%	0.07%	0.07%	0.22%	0.45%	0.30%	0.25%	0.08%	0.13%	0.11%	0.11%
Retro-diffusion - @ worst case	0.10%	0.10%	0.10%	0.10%	0.17%	0.17%	0.17%	0.17%	0.11%	0.11%	0.11%	0.11%
Total	0.16%	0.20%	0.17%	0.17%	0.39%	0.62%	0.47%	0.41%	0.19%	0.24%	0.22%	0.22%

Table 2 : Stray-light summary table for different contributors and different coating situations

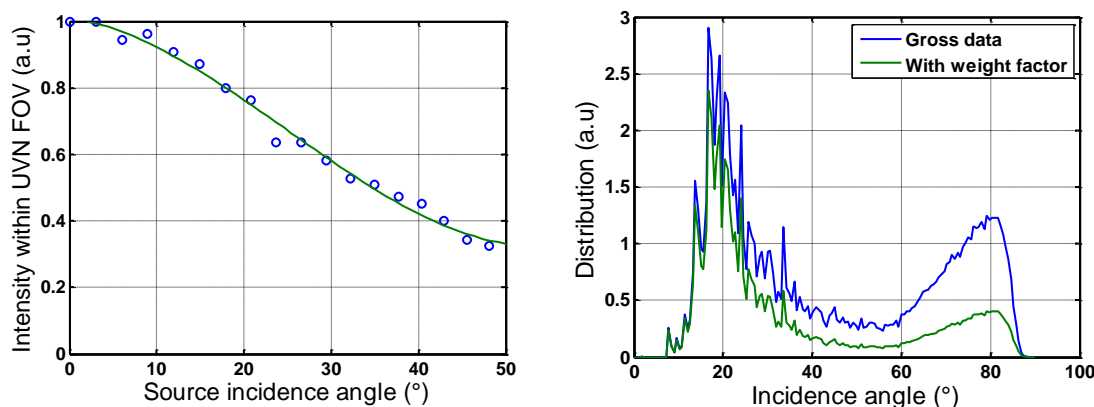


Figure 8: (left) Intensity of light diffused within UVN FOV as a function of the incidence angle on the diffuser. (Right) Angular distribution of the direct illumination stray-light, edges excluded, for vSun2 and hybrid coating. The weight factor is used to keep only the portion being diffused inside the UVN FOV.

Based on these results, the hybrid coating configuration was selected. Indeed, the black anodization alone doesn't give acceptable performance while acktar would overkill. The hybrid configuration, black anodization on the entire baffle except for acktar on the cone, is a good compromise in terms of performance and manufacturability. Finally, let's mention that earth shine stray-light was also investigated. The result gave negligible values of the stray-light, orders of magnitude below the sun stray-light.

III. EXPERIMENTAL CHARACTERIZATION

A. Facility and methods

The sun baffle stray-light rejection performance was experimentally characterized in the FOCAL 3 facility from the Space Center of Liège (Figure 9) [3]. The illumination is provided by a 2 meter focal length off axis parabola, exhibiting a 400mm beam diameter. A laser diode at wavelength 805nm is used at its focal plane. The UVN calibration assembly was placed on a manipulator, a hexapod from Symetrie®. This one performs accurate movements of the baffle with respect to the collimator, enabling the characterization of the UVN CAA at different fields.

The performance characterization was performed at the entrance pupil of the instrument. At that position, a lens was used to record on a detector the angular distribution of light. Due to experimental constraints, the distribution over the full UVN field of view ($X[^\circ] \times Y[^\circ] = \pm 2.1^\circ \times \pm 0.1059^\circ$) was obtained by stitching a set of 3 measurements done at overlapping angular ranges. In order to discriminate the sun stray-light from the nominal irradiance, a mask was used to occult the diffuser. With the mask, the stray-light due to the baffle is recorded on the detector while the nominal irradiance is blocked. The mask is placed on a translation and rotation stage to ensure that the entire entrance pupil is masked even when the hexapod is rotated. To measure nominal irradiance, the mask was removed. For the characterization of earth stray-light, the mask was also removed to fully illuminate the baffle and verify that no direct light hits the diffuser.

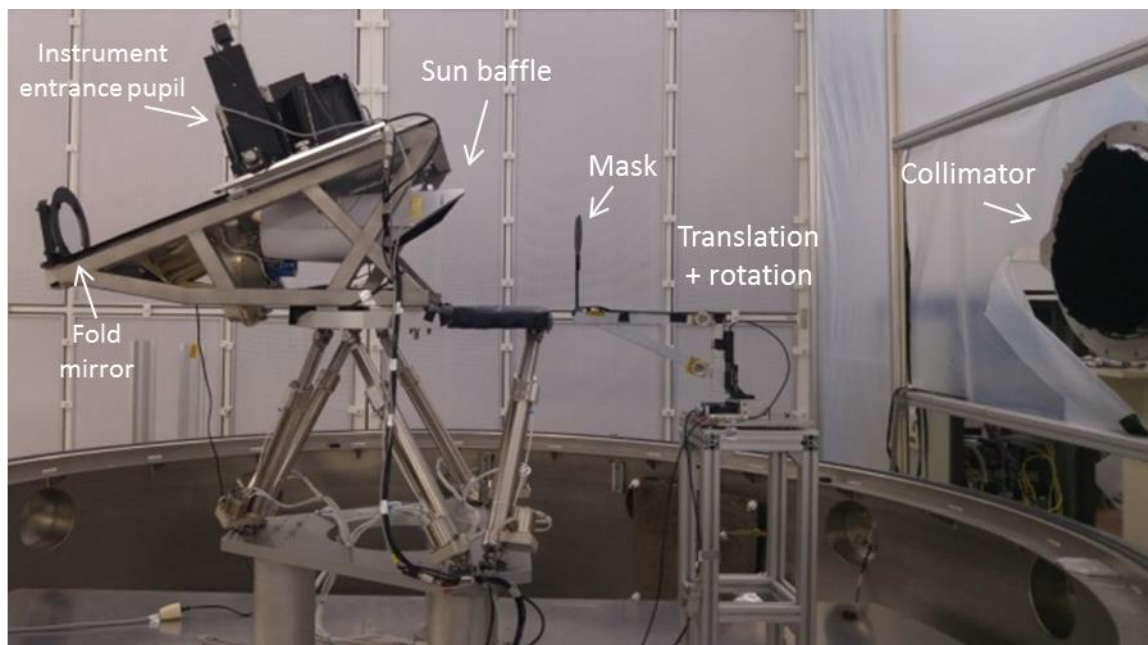


Figure 9: Experimental setup

The sun baffle stray-light calibration has been performed for 5 different fields, the fields vSun1 to vSun4 and the field normal to optical axis, vAxis (Table 1). The stray-light definition is the same as in the simulation, which is obtained by dividing the stray-light irradiance measurement to the nominal irradiance measurement. Similarly, for the sun baffle earthshine test, the stray-light was obtained by dividing the stray-light irradiance by the nominal irradiance measurement. The extreme of the earth field was considered in the measurement.

B. Results

Figure 10 shows a profile of the angular distribution of the sun stray-light as a function of the X axis field ($\pm 2.1^\circ$). Along the Y axis, the FOV is very small ($\pm 0.1059^\circ$) and the stray-light stays nearly constant. These results, summarized in Table 3, show that the stray-light rejection performance is within specifications. As predicted by theory, the stray-light rejection performance is the better for illumination along the optical axis (vAxis). Figure 10 shows that stray-light for vSun1 is higher than vSun2 and vSun4 is higher than vSun3, while simulations predicted the contrary. The difference is however small, it could come from the fact that the comparison was made for simulations prior to considering the angular weight factor which keeps only stray-light coming inside the field of view of UVN.

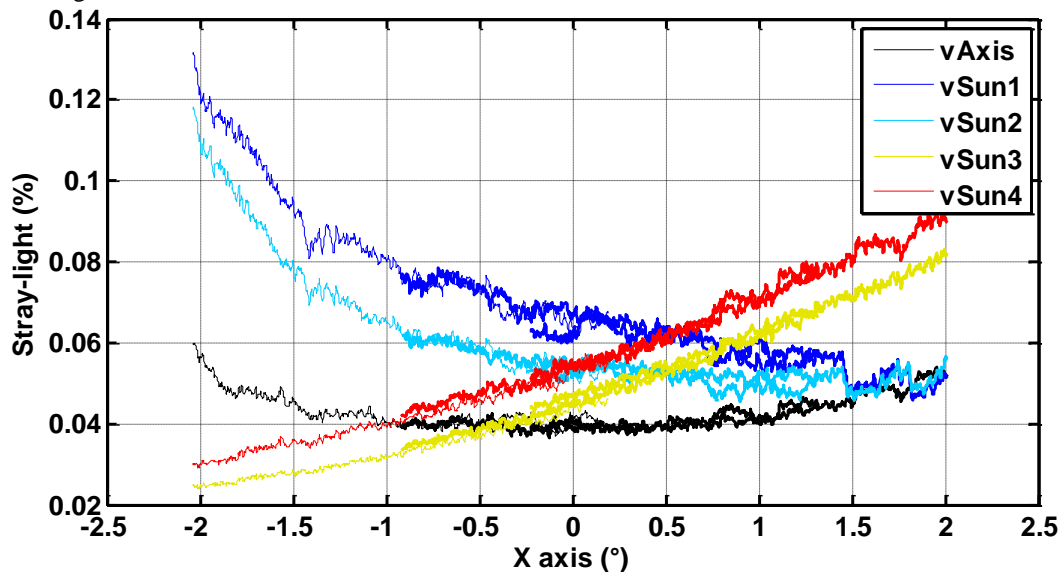


Figure 10: Experimental characterization of the stray-light for different configurations of sun illumination.

	Stray-light
VSun0	< 0.06% (average=0.04%)
VSun1	< 0.14% (average=0.07%)
VSun2	< 0.12% (average=0.06%)
VSun3	< 0.08% (average=0.05%)
VSun4	< 0.1% (average=0.06%)

Table 3: Experimental results of the sun baffle stray-light rejection performance

Earth shine characterization gave a stray-light below 0.0014%, much below the specification.

IV. CONCLUSIONS

A sun baffle has been designed, built and tested for the UVN embedded calibration assembly. The baffle has been designed to minimize the surfaces which are at the same time illuminated from the scene and seen from the detector. A stray-light analysis has been performed with the non-sequential ray-tracing software FRED and a coating trade-off has led to the decision of using inorganic black anodization coating on the entire baffle except for a cone at the bottom of the baffle which is akhtar coated. Experimental characterization has been performed in the clean room of the Space Center of Liège and confirms the stray-light rejection performance of the system.

ACKNOWLEDGMENT

This work has been supported by OHB/ESA in the frame of GMES Sentinel-4/UVN calibration assembly contract, GS4-KTH-UVN-CT-00001.

REFERENCES

- [1] <https://earth.esa.int/web/guest/missions/esa-future-missions/sentinel-4>
- [2] E.C. Fest, 2013, "Stray-light analysis and control". SPIE Press
- [3] E. Mazy et al., 2012, "Design and modelisation of a straylight facility for space optical instrument". Proc. SPIE 8550, Optical Systems Design, December 2012 Barcelona